The International Journal of Advanced Manufacturing Technology (2023) 129:2457–2474
https://doi.org/10.1007/s00170-023-12448-0

ORIGINAL ARTICLE

Theoretical and experimental research on a novel bending process for high-strength steel thin-walled tubes

Yanli Lin[1,2] · Shuo Wang[1,2] · Quan Qian[1,2] · Enqi Xu[1,2] · Zhubin He[1,2]

Received: 11 May 2023 / Accepted: 1 October 2023 / Published online: 16 October 2023

Abstract

To avoid wrinkling and cross-sectional distortion in thin-walled tube bending, a novel bending process called tube press bending under gas internal pressure (abbreviated as TGPB) is proposed. In the TGPB process, internal pressure serves a supportive function and generates an additional tensile stress, which can reduce the axial compressive stress on the inner side of the bend, avoiding the occurrence of wrinkles and cross-sectional distortions. Compared with the previous tube bending technologies, the support pressure inside the tube will not change suddenly with the volume change of the tube cavity due to the compressibility of gas. It is suitable for thin-walled tube bending with large, variable axial curvatures and high strength as the shape of the target part is determined by the die cavity. A theoretical prediction model of critical support pressure for TGPB without wrinkling defects is established. The critical support pressure, wall thickness, and section distortion of tubes with different curvatures bent by TGPB are analyzed through FE simulations and experiments, and tubes with different material properties are also done through FE simulations. The results indicate that the tube can be stably bent to the desired shape under the predicted critical support pressure, which is significantly affected by the bending radius and material characteristics, increases with strength coefficient, and decreases with bending radius and strain hardening exponent. A high-strength steel prebending part with complex variable axial curvatures has been successfully formed by TGPB technology under a support pressure of 5 MPa; the minimum and maximum bending radii of which are 846 mm and 2373 mm, respectively.

Keywords Thin-walled tube · Press bending under gas pressure · Critical support pressure · Wrinkling instability · Variable bending curvature

1 Introduction

Variable-section hollow components have been widely used in automotive manufacturing, aerospace, and other fields in recent years to meet the increasing demand for lightweight and energy saving [1, 2]. Hydroforming technology has significant advantages in the integral forming of thin-walled members with special-shaped cross sections. It is widely utilized in rockets, aircraft, and automobile industries. It can effectively reduce the weight and improve the strength of components [3–5]. Because the axis of the formed part is usually a curve, it is difficult to perform hydroforming directly on the original straight tube. Therefore, the original tube is necessary to be first bent into the same or similar axis shape as the target part through the prebending process before hydroforming [6]. However, the thin-walled tube is affected by multiple factors during the bending process and with a low axial stability. Defects such as wrinkles are prone to occur in the traditional bending process, making it difficult to meet the bending requirements of thin-walled tubes with variable curvatures and special-shaped cross sections [7].

Various tube bending technologies have been proposed to effectively avoid wrinkling defects in the tube bending process, including mandrel numerical control (NC) bending, mandrel push bending, filler bending, and hydrobending [8–11]. Computer numerical control (CNC) bending with mandrel is widely used, which prevents the occurrence of wrinkling and other defects by coordinating mandrels with other parts of the mold during the bending of tubes [12]. However, it is still difficult to bend ultra-high strength

✉ Zhubin He
hezb@dlut.edu.cn

1 School of Mechanical Engineering, Dalian University of Technology, Dalian 116024, China

2 State Key Laboratory of High-Performance Precision Manufacturing, Dalian 116024, China

thin-walled tubes such as titanium alloys with high strength and low hardening characteristics [13]. The push-bending with a flexible mandrel is suitable for single-elbow tubes but not multi-elbow tubes [14–16]. Filler bending requires adding solid media such as rosin, sand, or low melting temperature alloy to the tube before bending to avoid defects during the bending process. However, the pressure distribution is usually nonuniform, and the support pressure cannot be accurately controlled [17]. Fluids such as water or oil are used as filling media by some scholars for tube bending to achieve uniform support pressure and effectively avoid the damage to the inner wall of the tube caused by the medium [18]. However, the support pressure will suddenly rise or drop as the volume of the tube changes during the tube bending process, resulting in the occurrence of cracking or wrinkling [19], making it difficult to achieve real-time and accurate control of the support pressure.

Therefore, how to accurately predict the occurrence of wrinkling defects in the forming process has always been the goal pursued by scholars. Wang et al. [20] conducted hydrobending experiments and FE simulations on thin-walled aluminum alloy tubes and obtained the critical internal pressure of the tubes by combining simulations and experiments. However, this method of using FE simulations or multiple experiments to obtain critical internal pressure is not convenient or efficient in terms of cost and time. To achieve efficient and accurate prediction of wrinkling defects, some scholars have begun to use wrinkling critical judgment conditions to predict the forming results. Chen et al. [21] investigated the influence of blank holding force on the flange wrinkling of deep-drawing process through combined experimental, numerical, and reduced-order modeling approaches. Chen et al. [22] proposed a theoretical prediction model based on the critical wrinkling stress criterion, which quantitatively predicted the wrinkling of unsupported areas of curved thin-walled shells in sheet hydroforming. The influence of the reverse bulging effect on the critical hydraulic pressure and the hydraulic pressure on the critical wrinkling stress is analyzed, and the critical loading path of hydroforming is established. In the tube forming process, Chu et al. [23, 24] analyzed the wrinkling of the tube side wall in hydroforging, established a wrinkling defect prediction model based on a critical condition of support pressure, and achieved the prediction of critical support pressure of wrinkling during tube hydroforging. In addition, Wang and Cao [25] proposed a theoretical prediction method for minimum bending radius of CNC tube bending on the basis of the critical condition of the work done by the membrane force during the bending process. Based on the research conducted by Wang and Cao, Yang and Li [26, 27] further considered the influence of boundary conditions during CNC tube bending, established a critical wrinkling prediction model with higher prediction accuracy, and verified its accuracy through FE analysis.

To sum up, CNC bending and hydrobending are the two main technologies for bending thin-walled tube, and research on the wrinkling behavior of tubes is mainly focused on these two technologies. However, thin-walled tubes with a variable axis curvature or high strength are difficult to be bent through the CNC bending process, and serious wrinkling defects are prone to develop during bending. Regarding the tube hydrobending, changes in the volume of the tube cavity or liquid leakage can cause a sudden rise or drop in the support pressure, causing tube rupture or wrinkling.

In this paper, a novel bending process called tube press bending under gas internal pressure (abbreviated as TGPB) is proposed to achieve thin-walled tube bending without wrinkling defects. Firstly, the wrinkling defects of tube bending under support pressure are theoretically analyzed, and the theoretical model of critical support pressure is established. The critical support pressure for high-strength steel tube with different curvatures is calculated theoretically using the proposed model, and the results of which agree very favorably with the experiments and FE analysis. Then, the critical support pressure, wall thickness, and section distortion of tubes with different curvatures bent by TGPB are analyzed through analysis and experiments, and tubes with different material properties are also done through FE analysis. Finally, the TGPB technology is applied to successfully bend a thin-walled tube of high-strength steel with complex variable axial curvatures.

2 Tube gas press bending (TGPB)

2.1 Principle of TGPB

Combining the advantages of forming under support pressure and the characteristic of gas compressibility, a tube press bending technique under the support of gas pressure is proposed, which is called tube gas press bending (abbreviated as TGPB), as shown in Fig. 1. The two ends of the tube are closed, and an additional axial tensile stress will be generated under the support pressure, which can reduce the axial compressive stress on the inner side of the tube, thereby effectively suppressing wrinkling and cross-sectional distortion defects. At the same time, due to the compressibility of gas, the support pressure inside the tube will not change suddenly with the volume change of the tube cavity during the TGPB process, which is different from the previous bending technologies using solid and liquid media.

The specific process of TGPB is as follows: prior to bending, the two ends of the tube are sealed first, and the sealed tube is inflated by a high-pressure gas source. The internal gas pressure of the tube is accurately controlled in real time by the pressure control system so that the tube can be successfully bent without wrinkling defects under the

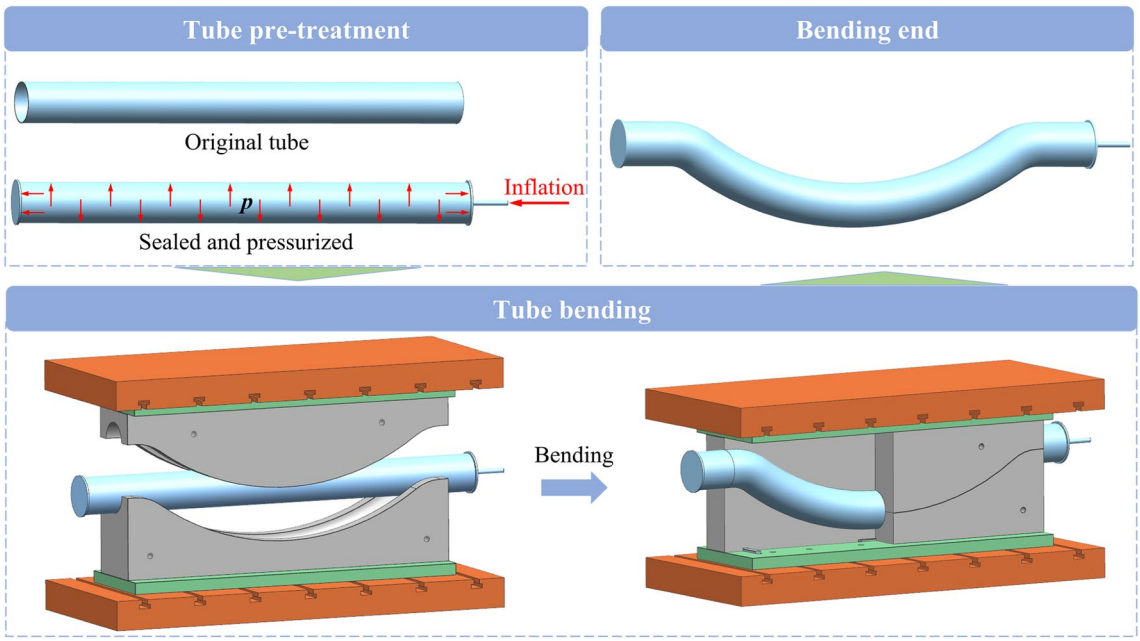

Fig. 1 Schematic of TGPB

combined actions of the predetermined support pressure and the clamping force provided by a hydraulic press.

Compared to the previous tube bending technologies, the TGPB technology proposed in this paper has the following unique advantages:

(1) The internal pressure serves a supportive function and generates an additional tensile stress, which can reduce the axial compressive stress on the inner side of the bend and avoid wrinkles and cross-sectional distortions, thereby increasing the bending limit and obtaining a smaller bending radius.
(2) It is suitable for thin-walled tube bending with large, variable axial curvatures and even high strength as the shape of the target part is determined by the die cavity.
(3) The support pressure will not suddenly change due to the volume change of the tube cavity during deformation or the gas leakage, and the pressure distribution is uniform and easy to control during bending.
(4) The gas medium will not cause damage to the inner wall of the tube.

2.2 Theoretical model of critical support pressure

The support pressure has a significant impact on tube bending. If the support pressure is insufficient, wrinkling defects will not be suppressed. Conversely, if the support pressure is too high, rupture will happen. Therefore, accurate prediction of the critical support pressure is of great importance for TGPB experiments.

In the process of plastic deformation of tubes, the deformation is highly complex. Therefore, it is necessary to make certain assumptions and approximations when conducting theoretical analysis and numerical simulations. Firstly, it is assumed that the material properties of the tube are isotropic, meaning that the material properties are the same in all directions. Secondly, during the bending process, it is assumed that the loading stress state remains essentially unchanged, allowing for the approximate adoption of the total form of plastic strains. These assumptions and approximations enable us to simplify the problem and facilitate effective analysis and simulation.

Wrinkling defects may occur when the tube is bent to a certain radius of curvature, as shown in Fig. 2. The support pressure has an inhibitory effect on the wrinkling of the tube in the TGPB process. According to the energy method [28], when the tube does not experience wrinkling defects, the work W_p done by the support pressure needs to satisfy the following conditions:

$$W_p \geq E_p - E_0 \tag{1}$$

where E_p is the plastic strain energy when the tube is deformed to a predetermined bending radius under support pressure without wrinkling defects and E_0 is the plastic strain energy when the tube is deformed to a predetermined bending radius with wrinkling defects under no support pressure.

The shape of the wrinkling area often presents an approximate periodic fluctuation, which is commonly described in the form of a cosine function [26, 29]. By

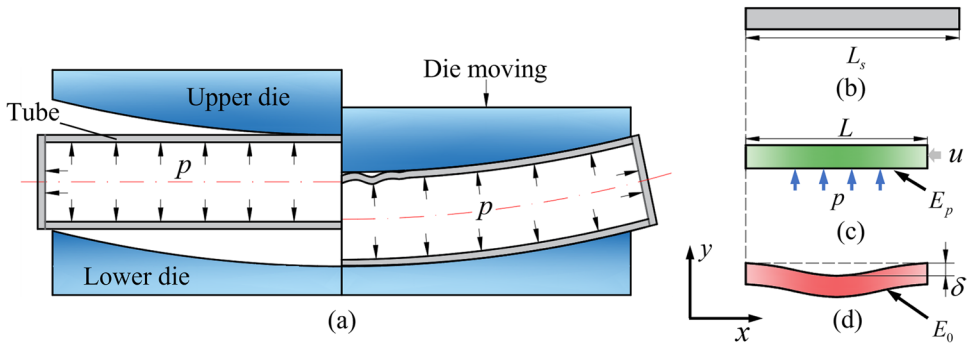

Fig. 2 Geometric model of TGPB. **a** Wrinkling diagram of tube bending. **b** Initial state of the inner side. **c** Ideal compression state of the inner side. **d** Wrinkled state of the inner side

analyzing the micro-element on the tube wall, the shape of the tube wrinkling can be approximated as follows:

$$y = \frac{\delta}{2}(1 - \cos mx) \tag{2}$$

where y is the wrinkling wave function, x is the axial displacement of the tube, δ is the maximum wave height of the wrinkling area, and m is the corresponding frequency of the waveform.

Using 2π as a period, the waveform frequency m can be expressed as

$$m = \frac{2\pi}{L} \tag{3}$$

where L is the wavelength of the wrinkling area.

The initial length of the small element is assumed as L_s, and when the axial compression $u$is applied, the compression strain can be expressed as

$$\varepsilon_c = -\ln\left(\frac{L_s - u}{L_s}\right) \tag{4}$$

Assuming that the arc length at the neutral layer position of the tube remains constant in the compressed and wrinkled state on the inner side of the bend, according to the curve arc length formula, the initial length L_s of the micro-element before bending is

$$L_s = \int_0^L \sqrt{1 + y'^2}dx \approx \int_0^L 1 + \frac{1}{2}y'^2 dx \tag{5}$$

According to Eqs. (2), (3), (4), and (5), the maximum wave height δ in the wrinkling area can be derived as follows:

$$\delta = \sqrt{\frac{4uL}{\pi^2}} = \frac{2L_s}{\pi}\sqrt{e^{-\varepsilon_c} - e^{-2\varepsilon_c}} \tag{6}$$

The work [29] W_p produced by the supporting internal pressure p is

$$W_p = p\frac{2\delta L_s}{3} \tag{7}$$

According to Eq. (1) and Eq. (7), to prevent the tube from wrinkling defects, the support pressure should meet the following:

$$p \geq \frac{3\left(E_p - E_0\right)}{2\delta L_s} \tag{8}$$

The critical support pressure P_{cr} without wrinkling for TGPB technology is

$$p_{cr} = \frac{3\left(E_p - E_0\right)}{2\delta L_s} \tag{9}$$

Assuming that there is no cross-sectional distortion during the tube bending process, the circumferential deformation can be neglected, and the tube diameter also remains unchanged. The radial strain component ε_t, the circumferential strain component ε_θ, and the axial strain component ε_z are as follows:

$$\begin{cases} \varepsilon_\theta = 0 \\ \varepsilon_t = -\varepsilon_z \\ \varepsilon_z = -\varepsilon_c \end{cases} \tag{10}$$

Assuming the material satisfies the Mises yield criterion and the hardening law of which can be described in power exponential form, the corresponding equivalent strain $\overline{\varepsilon}$ and equivalent stress $\overline{\sigma}$ can be described as

$$\begin{cases} \overline{\varepsilon} = \frac{\sqrt{2}}{3}\sqrt{\left(\varepsilon_z - \varepsilon_\theta\right)^2 + \left(\varepsilon_t - \varepsilon_\theta\right)^2 + \left(\varepsilon_z - \varepsilon_t\right)^2} \\ \overline{\sigma} = K\overline{\varepsilon}^n \end{cases} \tag{11}$$

where K is the strength coefficient and n is the strain-hardening exponent.

The volume of unit width micro-element is assumed as constant before and after bending, and the volume can be expressed as

$$V = L_s t_0 \cdot 1 \tag{12}$$

where t_0 is the initial thickness of the tube.

The plastic strain energy of the tube deformed to a predetermined bending radius without wrinkling defects under a support pressure can be calculated as

$$E_p = \iiint \bar{\sigma} d\bar{\varepsilon} dV = \frac{K L_s t_0}{n+1}\left(\frac{-2}{\sqrt{3}}\varepsilon_c\right)^{n+1} \tag{13}$$

The plastic strain energy of the tube deformed to a predetermined bending radius with wrinkling defects under no support pressure [30] is

$$E_0 = \frac{2Kt_0}{n+1}\left(\frac{t_0}{\sqrt{3}}\right)^{n+1}\left(\frac{2}{m^2\delta}+\frac{t_0}{2}\right)^{-n}\operatorname{atan}\left(\frac{m\delta}{2}\right) \tag{14}$$

To reduce the correlation of independent variables and the complexity of the relation expression, $\lambda = L_s/t_0$ is defined. λ is a positive real number. Therefore, the critical support pressure without wrinkling defects can be described as

$$p_{cr} = \frac{3K\pi\left(e^{\varepsilon_c}-e^{2\varepsilon_c}\right)^{-1/2}}{4\lambda(n+1)}\left(\left(\frac{-2}{\sqrt{3}}\varepsilon_c\right)^{n+1} - \frac{2}{\lambda}\left(\frac{1}{\sqrt{3}}\right)^{n+1}\left(\frac{\lambda}{4\pi\sqrt{e^{\varepsilon_c}-e^{2\varepsilon_c}}}+\frac{1}{2}\right)^{-n}\arctan\left(2\sqrt{e^{-\varepsilon_c}-1}\right)\right) \tag{15}$$

considering the shift of the strain neutral layer in the bending. The relative bending radius of the tube is defined as $\alpha = R/r$. According to Eq. (16), the axial compressive strain on the inner side of the tube during bending can be described as

$$\varepsilon_c = \ln\left(\sqrt{\frac{\alpha-1}{\alpha+1}}\right) \tag{17}$$

However, it should be noted that the cross section of the tube during bending will show the characteristics of thinning of the outer wall thickness and thickening of the inner wall thickness. Additionally, the strain-neutral layer will shift towards the center of the bend [31], as shown in Fig. 3. Therefore, it is necessary to consider the strain-neutral layer shift [32], and the corresponding ε_c of which can be expressed as

$$\begin{cases} \varepsilon_c = \ln\left(\frac{R - r\cos\theta}{R'}\right) \\ R' = r\sqrt{\left(\frac{R}{r}\right)^2 - 1} \end{cases} \tag{16}$$

where R is the tube bending radius, r is the initial tube radius, R' is the bending radius after neutral layer shift, and θ is the angle corresponding to any position on the cross section A-A of tube.

The axial compressive strain at $\theta = 0°$ position on the tube cross section is maximum during the tube bending process. If there is no wrinkling defect at the 0° position, it can be considered that the wrinkling defect will not develop on the inner side of the tube. Therefore, the axial strain at the 0° position can be used as the axial compressive strain on the inside of the tube to predict the critical support pressure

Therefore, the critical support pressure of the TGPB considering the strain-neutral layer shift during bending can be expressed as

$$p_{cr} = \frac{3K\pi\left(\sqrt{\frac{\alpha-1}{\alpha+1}}-\frac{\alpha-1}{\alpha+1}\right)^{-1/2}}{4\lambda(n+1)}\left(\begin{array}{c}\left(\frac{-2}{\sqrt{3}}\ln\left(\sqrt{\frac{\alpha-1}{\alpha+1}}\right)\right)^{n+1} \\ -\frac{2}{\lambda}\left(\frac{1}{\sqrt{3}}\right)^{n+1}\left(\frac{\lambda}{4\pi\sqrt{\frac{\alpha-1}{\alpha+1}-\frac{\alpha-1}{\alpha+1}}}+\frac{1}{2}\right)^{-n} \\ \arctan\left(2\sqrt{\sqrt{\frac{\alpha+1}{\alpha-1}}-1}\right)\end{array}\right) \tag{18}$$

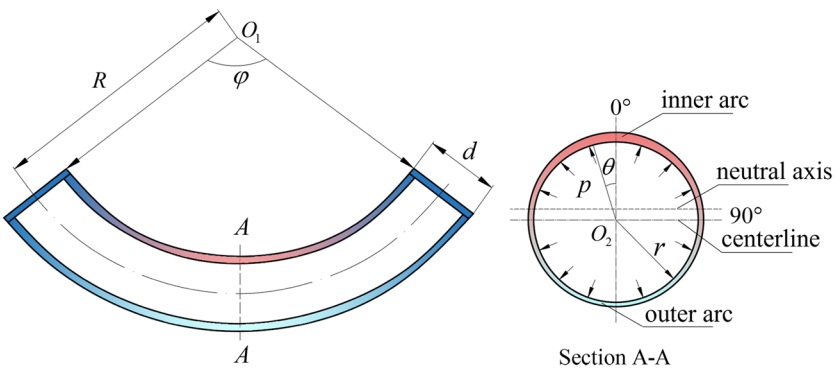

Fig. 3 Bending geometry and cross section of the tube

From Eq. (18), the critical wrinkling support pressure for TGPB is a function of K, n, α, and λ, while α is determined by the tube bending radius R and the initial tube radius r. λ is determined by the initial length of the micro-element L_s and the initial tube thickness t_0. Once the material and initial dimensions of the tube are determined, the critical support pressure is only related to the bending radius R and the initial length of the micro-element L_s. L_s is related to the wrinkling of the tube bending, which can be approximately considered as the length of the wrinkling area without support pressure. However, the wrinkling parameters of the tube bending without a support pressure cannot be foreseen in advance. So, the critical support pressure p_{cr} cannot be determined directly by Eq. (18). Considering that the length L_s in bending is much smaller than the length L_f of deformation area, that is, $0<\lambda<L_f/t_0$, the solution of the critical support pressure p_{cr} can be transformed into the solution of the following optimization problem:

$$\begin{aligned} &\max \quad p_{cr}(\lambda) \\ &\text{s.t.} \quad \lambda \in \left(0 \;\; L_f/t_0\right) \\ &\qquad \alpha = R/r \end{aligned} \tag{19}$$

When the parameters consisting of performance and initial dimensions of tube and bending radius are given, the maximum value of p_{cr} at $\lambda \in \left(0 \;\; L_f/t_0\right)$ can be used as the final critical support pressure for TGPB. Once the internal pressure exceeds the critical pressure, regardless of the value of λ, the tube will not experience wrinkling defects. Theoretically, p_{cr} takes the extreme values at $\partial p_{cr}/\partial\lambda=0$; in practice, the maximum value of p_{cr} at $\lambda \in \left(0 \;\; L_f/t_0\right)$ can be solved by common numerical algorithms such as the nonlinear least squares method.

3 Materials and methods

3.1 Experimental materials

High-strength steel BR1500HS thin-walled tube is used as the experimental tube with a nominal wall thickness of 1.2 mm and an outer diameter of 64 mm. The initial tube length for experiment is 700 mm, with the bending region length of 580 mm. All tubes are from the same batch.

The UT experiments are performed on ASTM E8 standard specimens which are cut from the tube along the axial direction. The test is performed thrice, and the true stress-strain curves fitted by power-exponent hardening model ($\overline{\sigma} = K\overline{\varepsilon}^n$) are shown in Fig. 4. The K and n values are adjusted by the least square method to make the square error minimum.

The elastic modulus E, Poisson's ratio ν, yield strength σ_s, tensile strength σ_b, strength coefficient K, and strain hardening exponent n of BR1500HS tube are shown in Table 1.

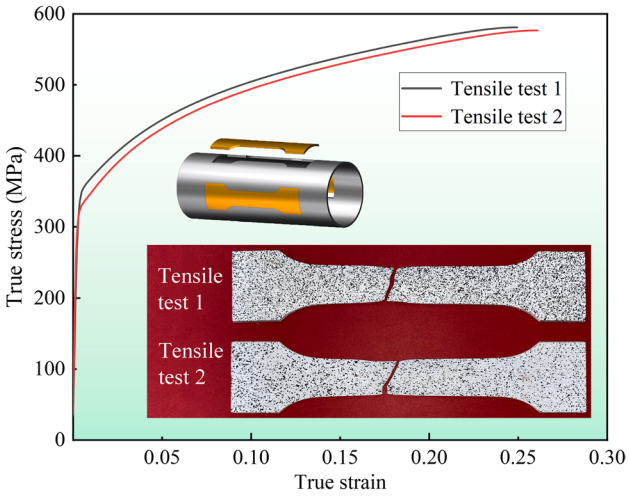

Fig. 4 True stress-strain curve of the BR1500HS tube

Table 1 Mechanical property parameters of BR1500HS

E (GPa)	Poisson's ratio v	Yield strength σ_s (MPa)	Tensile strength σ_b (MPa)	Strength coefficient K (MPa)	Strain hardening exponent n
106	0.33	344.36	578.19	780.65	0.193

3.2 Experimental device and procedure

The experimental device of the TGPB is shown in Fig. 5. It consists of an upper die and a lower die, which are mounted on a 315-ton hydraulic press. The displacement control accuracy is 0.1 mm, and the gas pressure control accuracy is 0.1 MPa.

Before conducting the TGPB experiments, the two ends of the tube are sealed by welding through end cover. One end of the tube is fully sealed, while the other end is connected to the high-pressure gas source through the stainless-steel high-pressure gas tube. The support pressure inside the tube is accurately controlled by the internal pressure control system. The experimental process of TGPB is shown in Fig. 6.

During the experiments, the tube specimen is first placed in the cavity of the lower die, and then, the press slider is controlled to move down until the upper die contacts the tube. Subsequently, the test specimen is inflated to reach the predetermined support pressure by the pressure control system. After that, the press slider is controlled to move down until the press bending process is completed. Finally, the press slider is controlled to move upward to facilitate taking

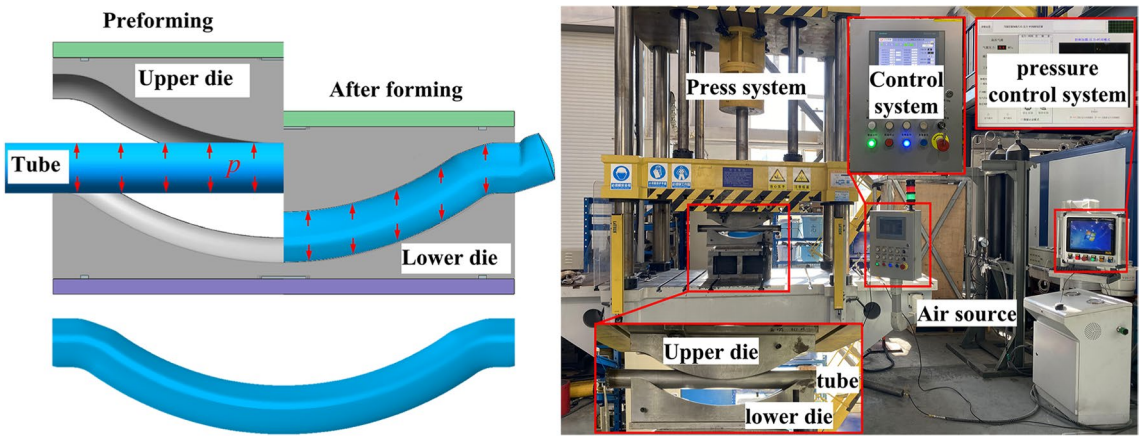

Fig. 5 Experimental device and experimental equipment

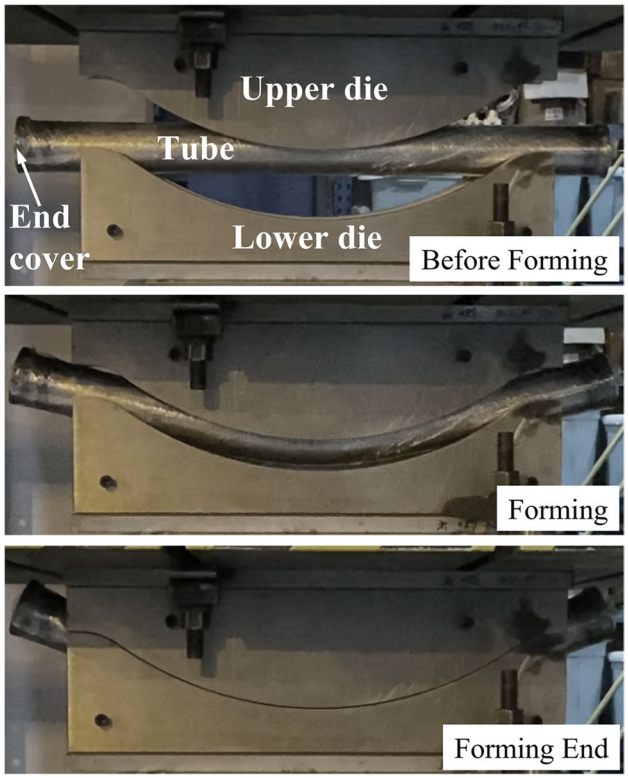

Fig. 6 The experimental process of TGPB

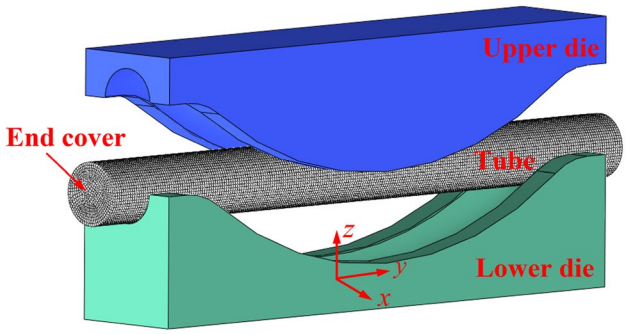

Fig. 7 The FE model of TGPB

out the bent tube, after the gas in the tube is discharged through a pressure relief valve.

3.3 Finite element model

Based on the principles of TGPB and material parameters of the tube, Abaqus is adopted to simulate the process of tube press bending. The finite element model mainly consists of three parts: tube with two end covers, upper die, and lower die, as shown in Fig. 7. Five integration points are defined in the tube thickness direction, and the tube is discretized with S4R elements. The upper and lower dies are set as three-dimensional discrete rigid bodies, with R3D4 quadrilateral elements. The tube is set to move freely without constraints. The lower die is completely fixed and constrained. The upper die is fixed in other directions and can only move up and down in the Z direction. The uniform pressure load is applied to the inside and both ends of the tube. The contacts between the upper die, the lower die, and the tube are all set as face-to-face, with a friction coefficient of 0.15.

4 Results and discussion

The theoretical prediction, simulation analysis, and experiments of TGPB on BR1500HS high-strength steel tubes with bending radii of 400 mm, 600 mm, and 800 mm are conducted. The causes of wrinkling are analyzed based on the results of experiments and FEM analysis, and the influence of material properties on the critical support pressure is discussed.

4.1 Theoretical calculation of critical support pressure

High-strength steel BR1500HS tube is taken as an example to illustrate the relationship between the critical support pressure p_{cr} and the relative bending radius α and λ, as shown in Fig. 8. The initial wall thickness and radius of the tube are not limited to specific values here. It can be seen that when the relative bending radius α is constant, the critical support pressure increases and then decreases with λ in a range of possible λ values, and there exists a maximum value. The maximum critical support pressure decreases as the relative bending radius α increases, which means that the required support pressure increases as the bending radius decreases once the initial radius of the tube is determined.

When the bending radius is 400 mm, 600 mm, and 800 mm, respectively, the relationship between the internal supporting pressure and λ is shown in Fig. 9. The corresponding relative bending radii α are 12.50, 18.75, and 25.00, respectively. The relationships of the support pressure with λ for different relative bending radii are consistent with Fig. 8. The maximum supported internal pressure decreases as the bending radius increases, and the critical support pressure p_{cr} of the high-strength steel BR1500HS tube corresponding to bending radii 400 mm, 600 mm, and 800 mm is 12.0 MPa, 7.1 MPa, and 4.9 MPa, respectively, as shown in Fig. 10.

4.2 Feasibility verification of TGPB

The feasibility of the proposed TGPB process is verified through FE simulations and experiments at different bending radii, and the effect of the support pressure on the wrinkling defects is analyzed. The FE simulations of TGPB with bending radii of 400 mm, 500 mm, 600 mm, 700 mm, and 800 mm had been conducted. For brevity, the results with a bending radius of 400 mm are presented herein as a representative case for specific analysis, while other simulation results are shown later in the paper.

The FE simulation results of tube press bending with different support pressures at 400 mm bending radius are shown in Fig. 11. The forming result is poor with no support pressure, and severe defects such as cross-sectional distortion, collapse, and wrinkles develop on the inner side of the tube after bending. When the support pressure is 4 MPa, the

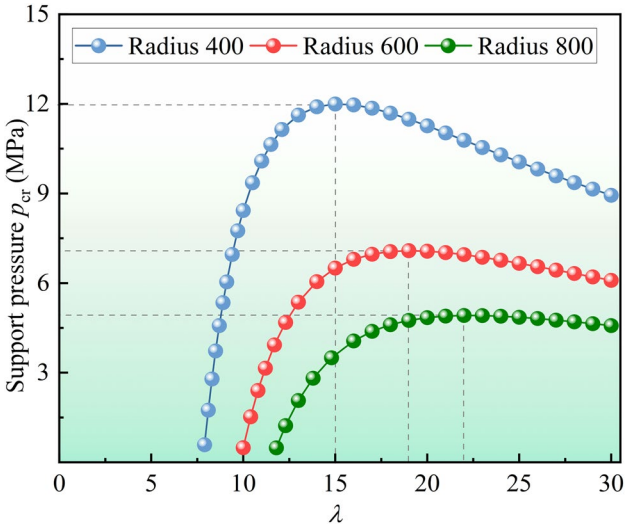

Fig. 9 Relationship between support pressure and λ (λ varies from 1 to 30)

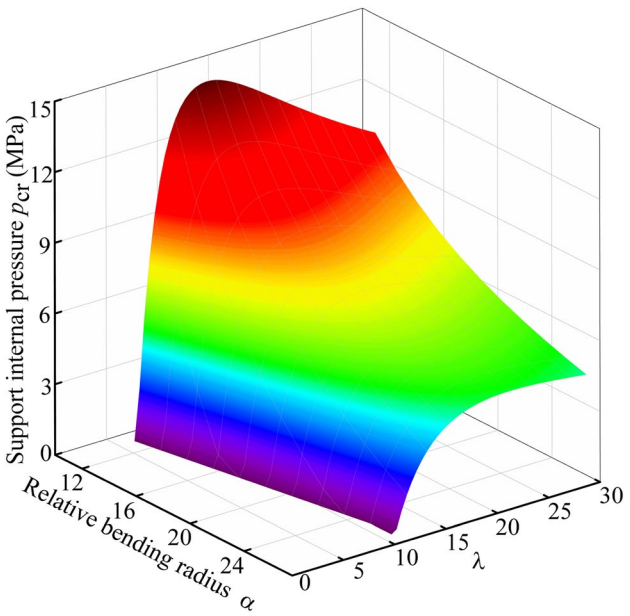

Fig. 8 The relationship between support internal pressure and relative bending radius α and λ

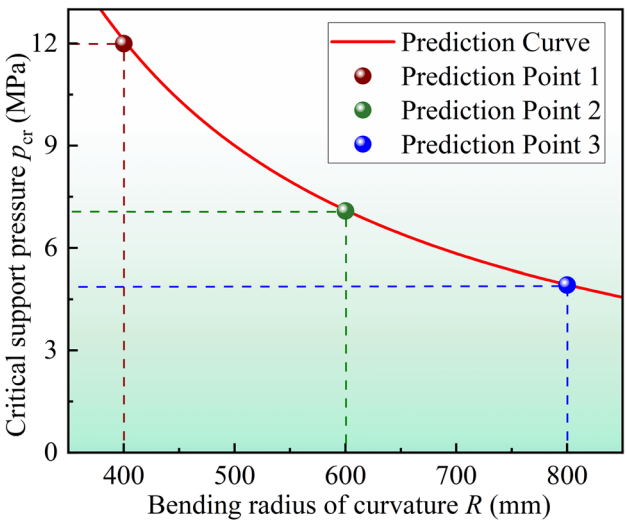

Fig. 10 Prediction curve of the theoretical model of critical support pressure in wrinkling

cross-sectional distortions disappear, but the tube still has severe wrinkling defects. When the support pressure reaches 8 MPa, there are only slight wrinkling defects on the inner side of the tube after bending. When the support pressure is 10 MPa, all wrinkling defects disappear from the inner side of the tube. When the support pressure is increased to 15 MPa, plastic deformation develops along the hoop direction, resulting in the extrusion of the tube from the die during the clamping process.

In fact, FE simulation results show that a small wavelength wrinkling develops on the inner side of the tube during the bending process with a support pressure of 10 MPa, but this wrinkling defect disappears when the die is completely closed. No wrinkling defect occurs during the bending process with a support pressure of 11 MPa. Therefore, 11 MPa is more suitable as the critical support pressure when the bending radius of tube is 400 mm in FE simulations, which is a little smaller than the theoretically predicted value of 12 MPa. Therefore, wrinkling defects will not arise under the theoretically predicted critical support pressure.

As the support pressure increases, the inhibitory effect on wrinkling defects becomes more pronounced, and the wavelength and wave height of the wrinkled area gradually decrease, until it reaches the critical support pressure, wrinkling disappears, and the tube is successfully bent without any defects. If the support pressure is too high, although there is no wrinkling defect, other defects such as flashing or even cracking may occur.

The TGPB experiments with different support pressures are performed on tubes with bending radii of 400 mm, 600 mm, and 800 mm, as shown in Fig. 12. For the experiments with a bending radius of 400 mm, severe wrinkling and collapse defects occur on the inner side of the tube without support pressure, while severe collapse defects occur on the outer side. When the support pressure is 2 MPa, the collapse on the outer side of the bend disappears, but there are still severe wrinkling and collapse defects on the inner side. When the support pressure is increased from 4 MPa to 8 MPa, only wrinkling defects remain on the inner side of the tube, and the wave height in the wrinkling area gradually decreases with the increase of the support pressure. When the support pressure reaches 10 MPa, the tube is perfectly bent with no defects. It can be seen from the experimental results that the minimum support pressure without wrinkling defects at bending radii of 400 mm, 600

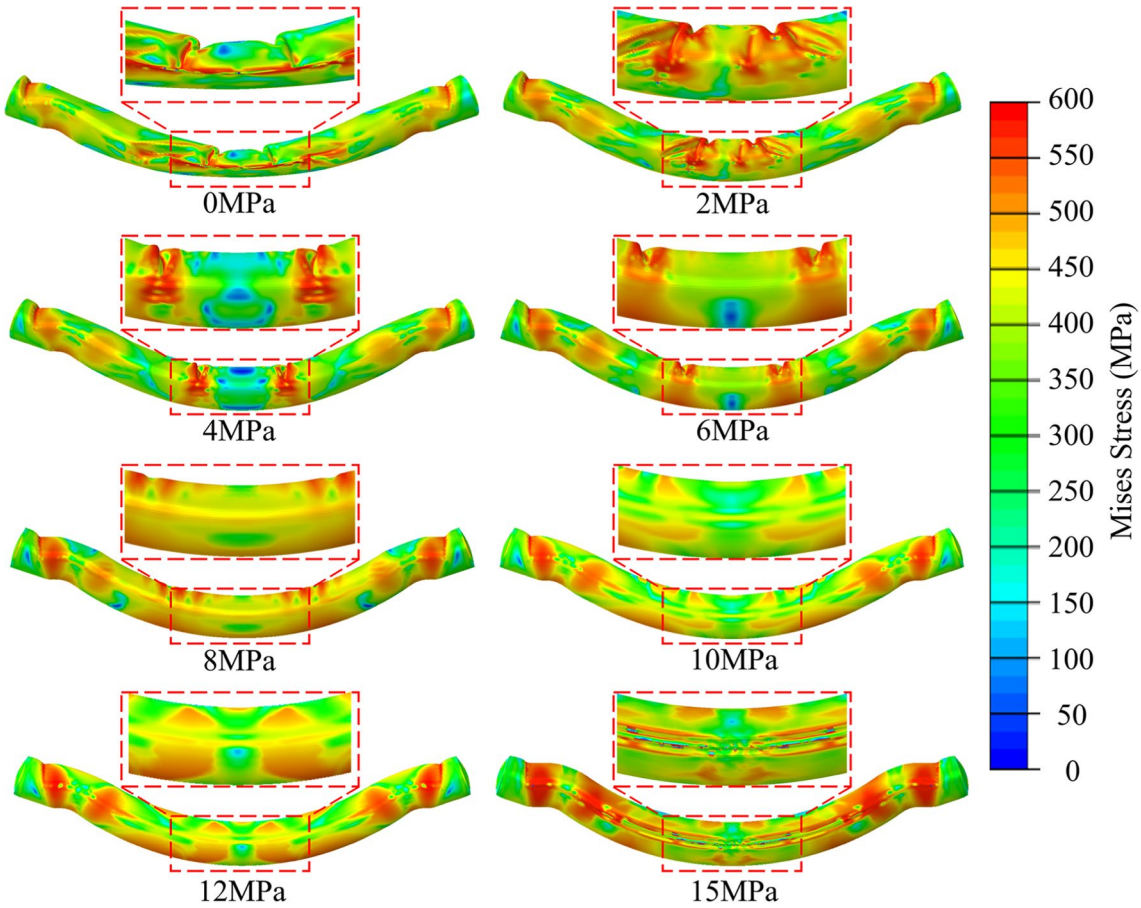

Fig. 11 Simulation results of tube press bending under different support pressure at $R = 400$ mm

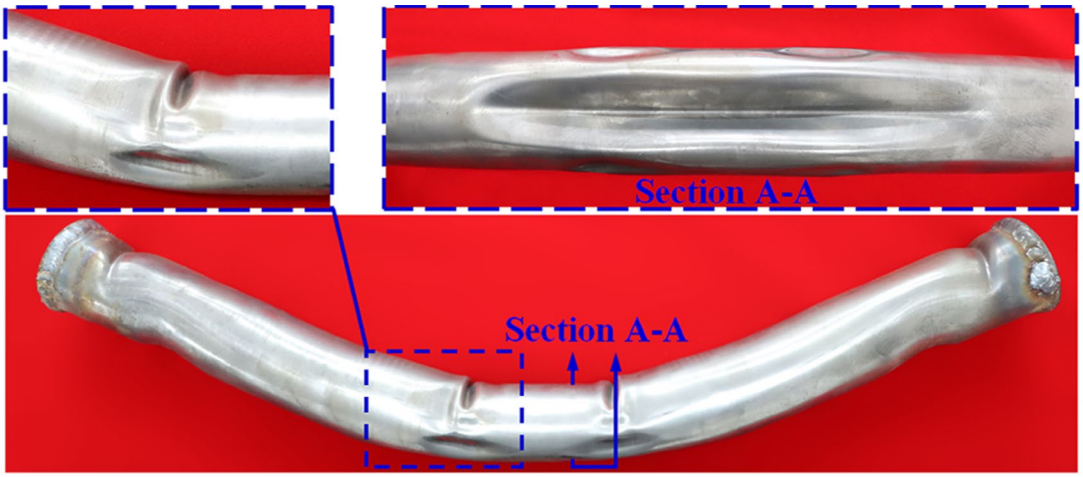

(a) bending radii 400 mm and support pressure 0 MPa

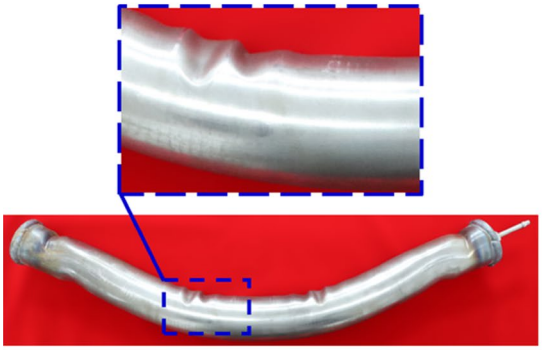

(b) bending radii 400 mm and support pressure 2 MPa

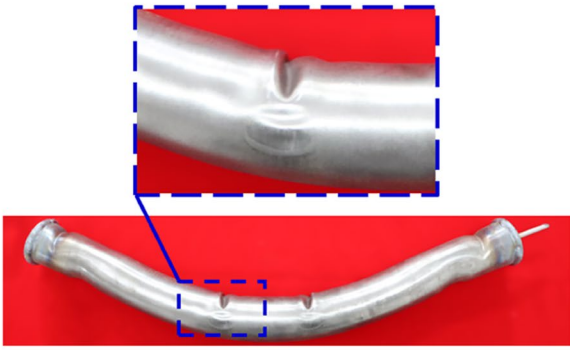

(c) bending radii 400 mm and support pressure 4 MPa

(d) bending radii 400 mm and support pressure 6 MPa

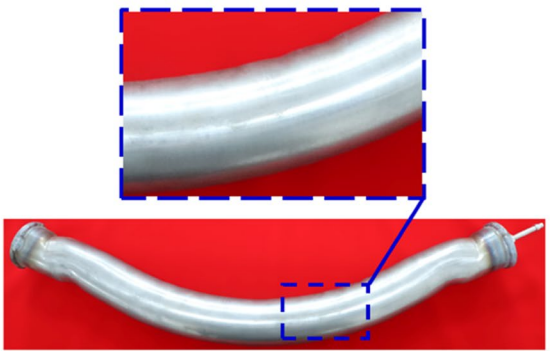

(e) bending radii 400 mm and support pressure 8 MPa

Fig. 12 Results of tube bending experiments with different bending radii and different support pressures

mm, and 800 mm is 10 MPa, 7 MPa, and 4 MPa, respectively, all of which are less than the theoretically predicted critical support pressures of 12 MPa, 7.1 MPa, and 4.9 MPa. This not only shows that the process of TGPB can achieve the tube bending without wrinkles but also shows that the established theoretical model of critical support pressure can be used for predicting the critical support pressure for TGPB.

Figure 13 compares the theoretical prediction of critical support pressure with the results of FE simulations and experiments for different bending radii. The theoretically predicted critical support pressure for different bending radii is slightly higher than the minimum support pressure without wrinkling defects obtained from the FE simulations and experiments, and the required critical support pressure increases with the decreases of bending radius. The maximum axial compressive strain in the cross section of the tube ($\theta = 0°$ position in Fig. 2) is used in the theoretical model of critical support pressure in Section 2.2 as the axial compressive strain ε_c on the inner side of the tube and ignores the friction between the tube and the die. In

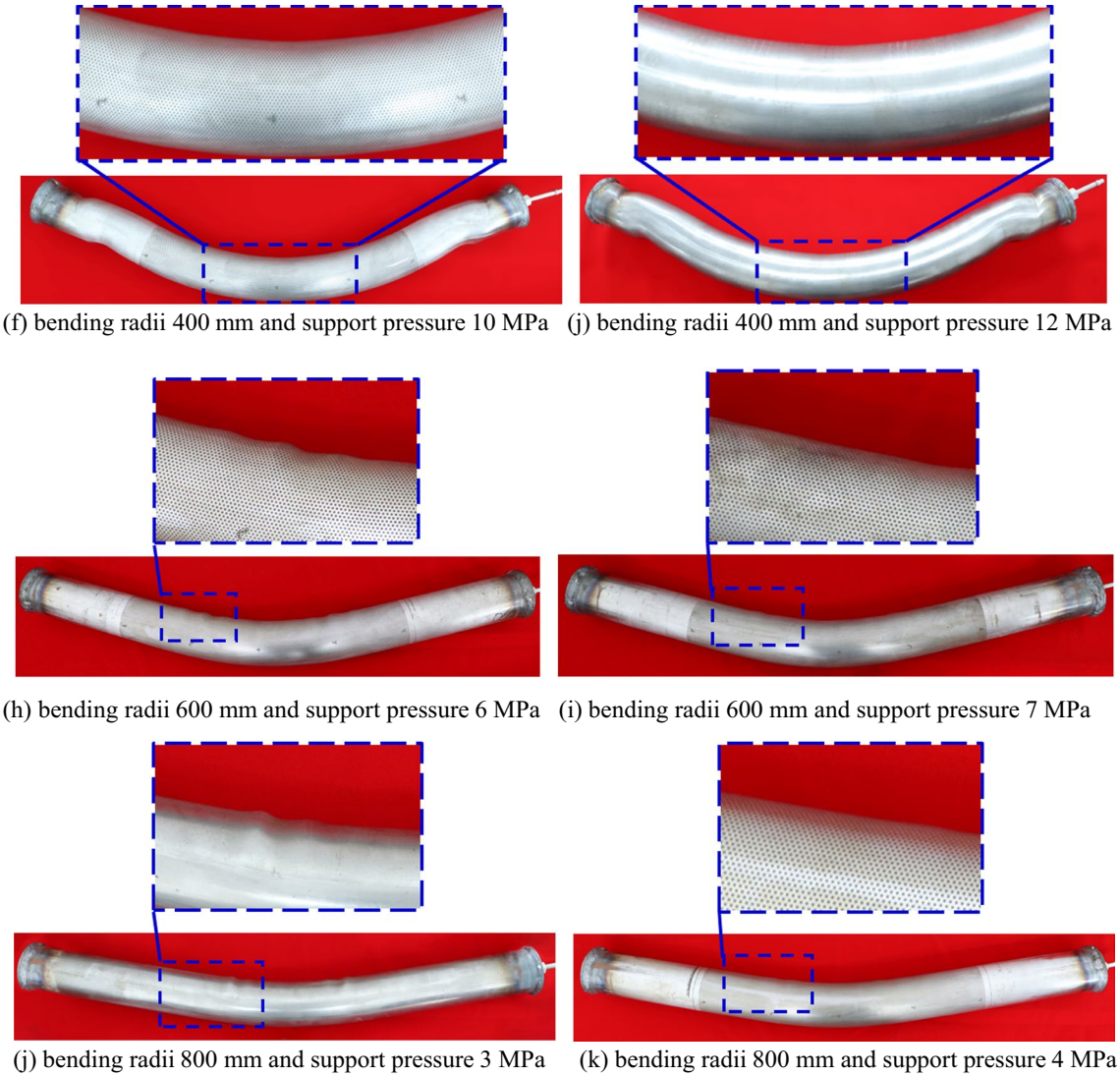

(f) bending radii 400 mm and support pressure 10 MPa (j) bending radii 400 mm and support pressure 12 MPa

(h) bending radii 600 mm and support pressure 6 MPa (i) bending radii 600 mm and support pressure 7 MPa

(j) bending radii 800 mm and support pressure 3 MPa (k) bending radii 800 mm and support pressure 4 MPa

Fig. 12 (continued)

the solving process, the maximum value of p_{cr} under a specific bending radius is used as the predicted critical support pressure for the tube bending. Therefore, the theoretical prediction of critical support pressure is a little higher than the true critical support pressure. Such theoretical prediction process is necessary because the goal is to achieve tube bending without wrinkling defects. If the theoretically predicted critical support pressure is smaller than the true value, the wrinkling defects will develop during the TGPB process using the theoretically predicted value.

4.3 Mechanism analysis of support pressure inhibiting wrinkling

The influence of support pressure on wrinkles and the causes of it during the bending process are analyzed through FE simulations. Figure 14 shows the distribution of axial stress developed during the TGPB process under different support pressures when the bending radius is 800 mm. It can be seen that axial compressive stress is generated on the inner side of the tube during the bending process, leading to axial compression deformation. When there is no support pressure or insufficient support pressure, the axial compressive stress is high, which exceeds the ultimate compressive stress that the material can undertake without losing stability, resulting in obvious wrinkling defects. When the support pressure is high enough, it can generate a considerable additional tensile stress along the axial direction of tube, which can reduce the axial compressive stress on the inner side of the tube, causing it to be lower than the ultimate compressive stress that the material can undertake. Therefore, no wrinkling defects will develop during the TGPB process. It can be further

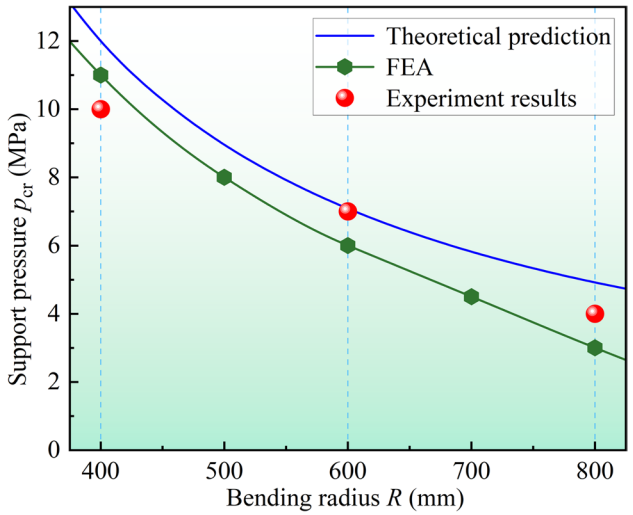

Fig. 13 Comparison of theoretical prediction p_{cr} with the results of FE simulations and experiments

concluded that as the bending radius decreases, the axial compressive stress on the inner side of the tube will increase, so a higher support pressure is required to completely suppress the wrinkling defects.

4.4 Effect of support pressure on the cross-sectional distortion

The effect of the support pressure on the cross-sectional distortion of the tube press bending is analyzed by FE simulations. Figure 15 shows the tube press bending cross section at different support pressures when the bending radius is 400 mm. When there is no pressure support, both the inner and outer sections of the tube are severely flattened and dented during bending, with flashing defects occurring at the clamping position. With the increase of the support pressure, the cross-sectional distortion of the outer side of the tube disappears, and the cross-sectional distortion of the inner side of the tube decreases. With the increase of the support pressure, the cross-sectional distortion of the outer side of the tube disappears, and the cross-sectional distortion of the inner side of the tube decreases. When the support pressure reaches the critical support pressure, the cross-sectional distortion on the inner side of the tube disappears, which is basically consistent with the initial cross-sectional shape of the tube. However, excessive support pressure can cause the tube to be extruded out of the die during clamping, resulting in flashing and cross-sectional distortion defects at the die-closing area.

To quantitatively characterize the degree of cross-sectional distortion of the tube, the cross-sectional out-of-roundness is defined as

$$\Delta_D = \frac{D_{\max} - D_{\min}}{D_0} \times 100\% \tag{20}$$

where $D_{\max}$ is the maximum outer diameter of the section after bending, $D_{\min}$ is the minimum outer diameter of the section after bending, and D_0 is the initial outer diameter of the tube.

Figure 16 shows the out-of-roundness of the cross section of the tube after bending under different support pressures. When there is no support pressure, the out-of-roundness of the cross section is 64.05% after tube bending with the most severe cross-sectional distortion. As the support pressure increases, the out-of-roundness of the cross section decreases gradually. When the support pressure increases to 10 MPa, the wrinkling defect disappears completely. At this time, the noncircularity of the cross section is reduced to 0.48%, and the shape of the cross section basically coincides with the initial cross section of the tube. The out-of-roundness decreases to 0.26% when the support pressure further increases to 12 MPa.

4.5 Effect of support pressure on wall thickness variation

During the tube bending process, the outer material is stretched along the axial direction, while the inner material is compressed in the axial direction. Under the influence of the axial tensile stress on the outer side during bending, the wall thickness of the tube becomes thinner. Conversely, under the influence of the axial compressive stress on the inner side during bending, the wall thickness of the tube increases. To reveal the influence of support pressure on the wall thickness of the inner and outer sides of the tube after bending, the wall thickness analysis of the innermost and outermost tube in FE simulations has been carried out at an analysis point every 2 mm along the axial direction.

Figure 17 shows the distribution of wall thickness on the inner side of the tube with a bending radius of 800 mm after bending under different support pressures. When the support pressure is 2 MPa, wrinkling defects occur on the inner side of the tube. Meanwhile, the wall thickness on the inner side thickens with a maximum thinning rate of −2.32%. As the support pressure increases to 4 MPa, the wrinkling defect on the inner side disappears with a maximum thickness thinning rate of −1.90%. The wall thickness thickening on the inner side of the tube will decrease as the support pressure increases. When the support pressure increases to 12 MPa, the wall thickness of the inner side changes from thickening to thinning, and the maximum thinning rate of the thickness is 1.25%. Compared with the case without support pressure, the support pressure can reduce the amount of wall thickness

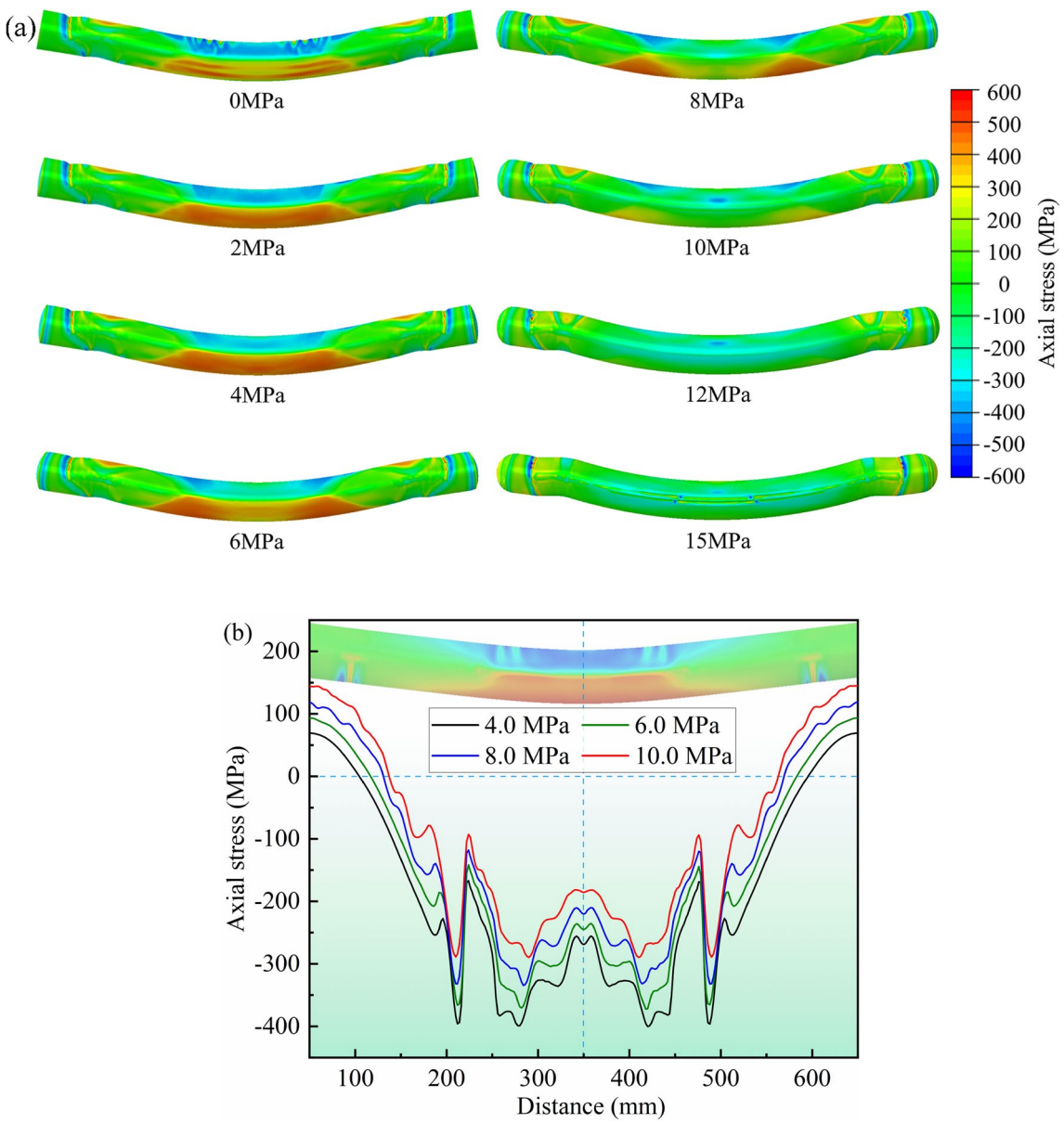

Fig. 14 Axial stress of tube bending under different support pressures. **a** Axial stress distribution contours. **b** Axial stress on the inner side of the tube

increase on the inner side of the tube, resulting in better forming performance.

Figure 18 shows the distribution of wall thickness on the outer side of a tube with a bending radius of 800 mm after bending under different support pressures. Regardless of whether there is support pressure, the wall thickness of the outer side of the tube is always in a state of thinning, and the amount of thinning increases as the support pressure increases. The maximum thickness thinning rates for support pressures of 2 MPa, 4 MPa, 6 MPa, 10 MPa, and 12 MPa are 2.52%, 2.99%, 3.61%, 5.15%, and 6.22%, respectively. When the support pressure is 4 MPa, no wrinkling defects are observed on the tube. Under this support pressure, the maximum thickness thinning rate on the outer side of the tube is 2.99%, with an actual thinning amount of 0.035 mm. Support pressure can effectively suppress wrinkling defects while reducing the amount of thinning on the outer side of the tube.

To characterize the uniformity of the variation of the tube wall thickness, the nonuniformity of the cross-sectional wall thickness is defined as

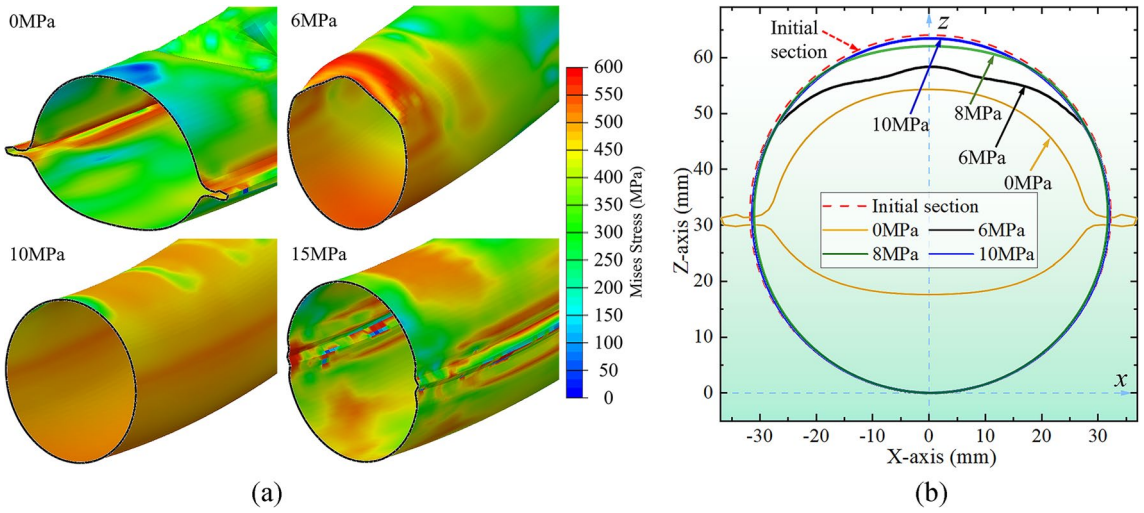

Fig. 15 Tube bending cross section with different support pressures. **a** Cross-sectional nephogram. **b** Cross-sectional shape

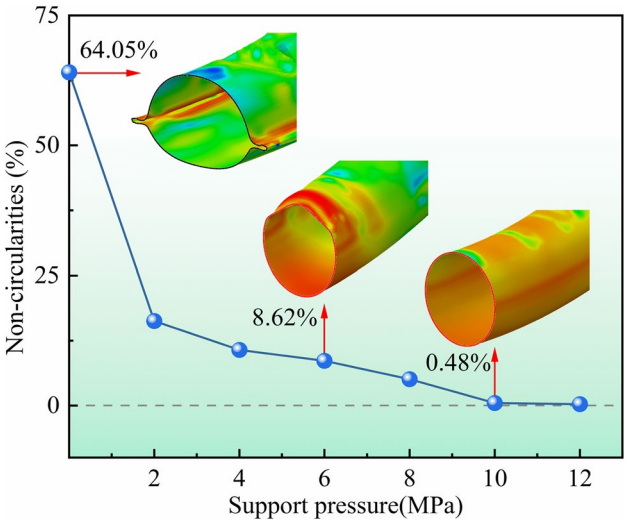

Fig. 16 Out-of-roundness of cross section under different support pressures

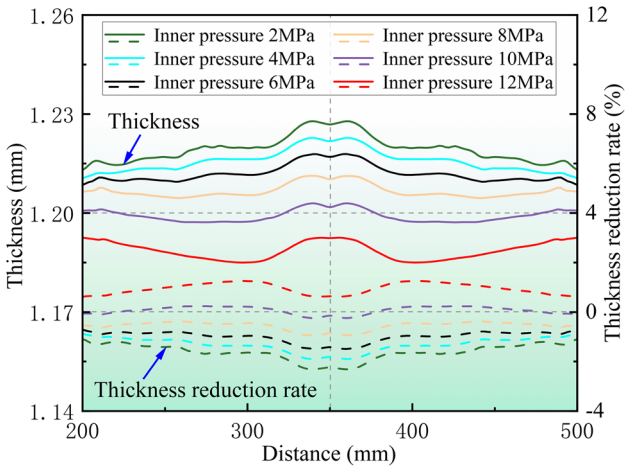

Fig. 17 Distribution of wall thickness and thickness thinning rate under different support pressures

$$\Delta_t = \frac{t_{\max} - t_{\min}}{t_0} \times 100\% \tag{21}$$

where t_{max} is the maximum wall thickness of the cross section after bending, t_{min} is the minimum wall thickness of the cross section after bending, and t_0 is the initial wall thickness of the tube.

Regardless of whether it is on the inner or outer side of the tube, the most significant variation in wall thickness is observed near the center of the tube. The wall thickness nonuniformity for support pressures of 2 MPa, 4 MPa, 6 MPa, 10 MPa, and 12 MPa is 4.84%, 4.89%, 5.10%, 5.39%, and 5.60%, respectively. Therefore, the increase of support pressure has little effect on the wall thickness nonuniformity of the tube cross section.

In addition, the characteristics of the thickness thickening of the inner side and the wall thickness thinning of the outer side of the tube shown by the FE simulation results verify that it is necessary to consider the axial compressive strain of the inner side of the tube in the strain-neutral layer shift in the theoretical prediction model of the critical support pressure in Section 2.2, which is also consistent with actual situations and can improve the accuracy of critical support pressure theoretical predictions.

4.6 Effect of material hardening properties on TGPB

The mechanical properties of the tube have a direct impact on its bending formability, and the critical support pressure

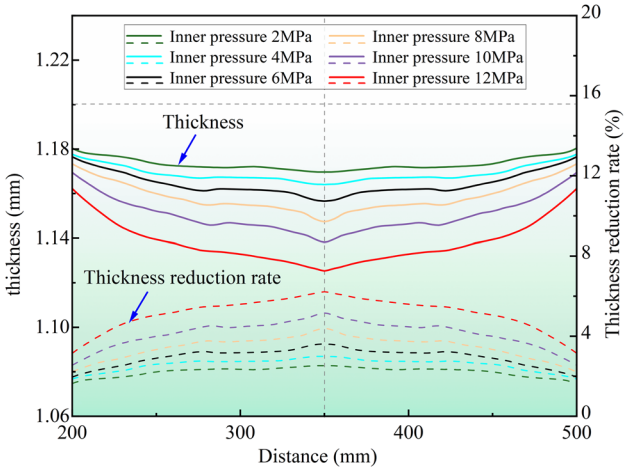

Fig. 18 The distribution of wall thickness and thickness reduction rate of the outer bending side under different support pressures

required for bending to the same radius of curvature varies with different materials. The critical support pressures of tubes with different strength coefficients K and strain hardening exponents n are predicted, as shown in Fig. 19. It can be observed that when bending to the same radius of curvature, the critical support pressure required increases with the strength coefficient increases, while decreases with the strain hardening exponent increases. Therefore, the critical support pressure is positively correlated with the material's strength coefficient and negatively correlated with the material's strain hardening exponent.

Figure 20 shows the axial stress distribution of the tube with different strength coefficients under the same bending radius and support pressure obtained through FE simulations. It can be observed from the figure that as the strength coefficient increases, the axial compressive stress on the inner side of the tube increases, which means that a higher support pressure is required to suppress the wrinkling defects, which is consistent with the results in Fig. 19.

Figure 21 shows the axial stress distribution of the tube with different strain hardening exponents under the same bending radius and support pressure obtained through FE simulations. It is evident that an increase in the strain hardening exponent leads to a decrease in the axial compressive stress on the inner side of the tube. Consequently, a lower support pressure is required to suppress the occurrence of wrinkling defects, which is also consistent with the results in Fig. 19.

4.7 Application of TGPB

The proposed TGPB technology is applied to the prebending component of A-pillar of a certain car model, which has a complex variable curvature in the axial direction, with a minimum bending radius of 846 mm and a maximum bending radius of 2373 mm. The tube used to form the component is identical in batch and specification to the experimental tubes described in Section 3.3. Figure 22 shows the 3D model of the prebending A-pillar component. Because the tube diameter to thickness ratio is large, which exceeds 53, the tube is highly prone to wrinkle in the bending process and difficult to be formed by CNC tube bending machine.

To successfully bend the component, it is first necessary to determine the critical support pressure without wrinkling defects. When the support pressure is insufficient, wrinkling defects cannot be completely suppressed. When the support pressure is too high, the tube will bulge and be extruded from the die during the clamping process. Therefore, the support pressure needs to be selected between the critical support pressure and the yielding pressure. According to the proposed theoretical model of critical support pressure, the smaller the bending radius, the larger the critical

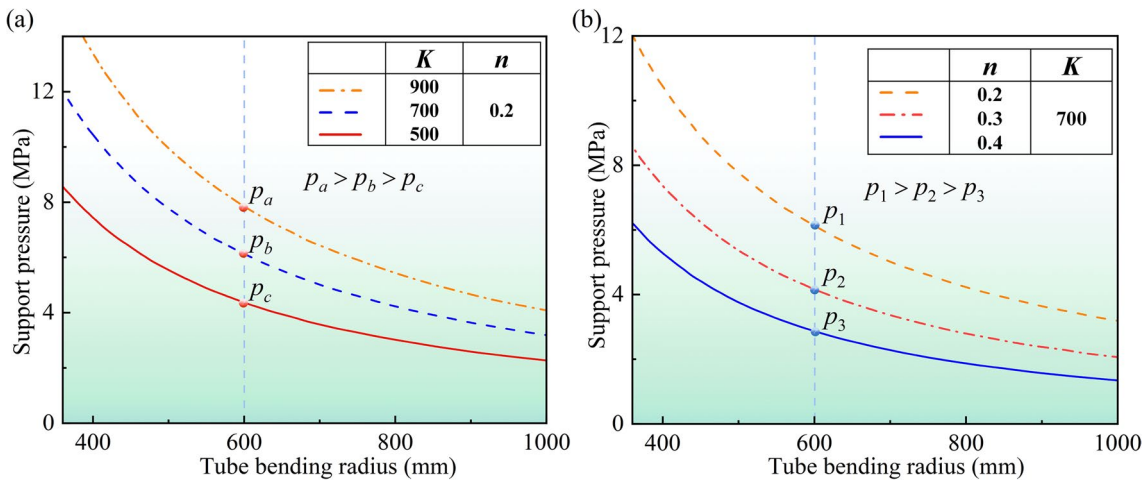

Fig. 19 Effect of material properties on critical wrinkling support pressure. **a** Different strength coefficients K. **b** Different hardening exponents n

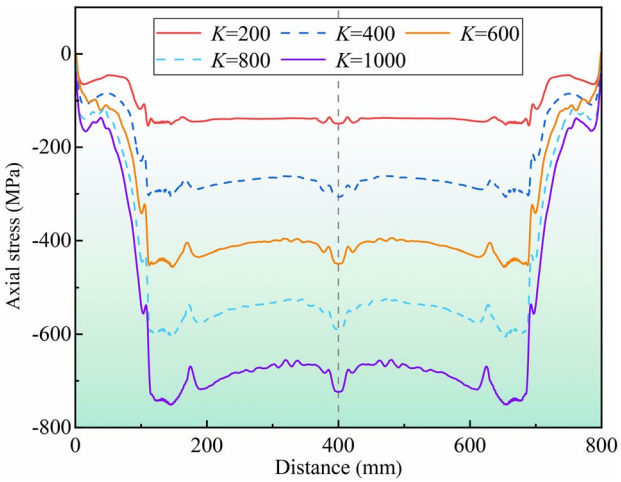

Fig. 20 Axial stress distribution on the inner bending side with different strength coefficients

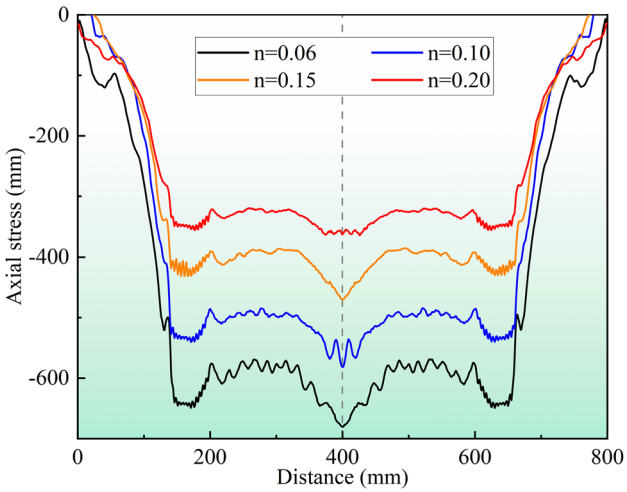

Fig. 21 Axial stress distribution on the inner bending side with different strain hardening exponents

support pressure required for tubes with the same material and size. Hence, the minimum bending radius of 846 mm is used to predict the required critical support pressure. As long as there is no wrinkling defect at the minimum bending radius, wrinkling defects will not occur at other locations. When the bending radius is 846 mm, the critical support pressure calculated is 4.58 MPa. Therefore, the required support pressure should not be less than 4.58 MPa when the prebending component is formed by TGPB technology.

FE simulations are conducted at the support pressure 4.0 MPa, 4.5 MPa, and 5.0 MPa, as shown in Fig. 23. It can be seen that slight wrinkling defects occur on the inner side of the tube when the support pressure is 4.0 MPa. However, the wrinkling defects completely disappear when the support pressure increases to 4.5 MPa. Therefore, using the theoretically calculated pressure of 4.58 MPa for tube press bending will successfully avoid the wrinkling defects.

The predicted critical support pressure is only the minimum required support pressure. Considering theoretical prediction errors, potential material inconsistency differences, and die effects, it is recommended to use a slightly higher support pressure than the theoretical prediction of the critical support pressure to ensure forming performance. Therefore, a support pressure of 5 MPa is used to form the prebending component shown in Fig. 22. As shown in Fig. 24, the bent tube has been successfully formed without wrinkling defects and meets the subsequent process requirements.

5 Conclusions

This paper proposes a novel bending process called TFPB, which is different from traditional solid medium-filling bending and hydrobending. Due to the compressibility of gas, the change in tube cavity volume during bending will not cause a sudden change in the support pressure, and the pressure distribution is uniform and easy to control. The most prominent feature is that it is suitable for bending thin-walled tubes with large, variable axial curvatures and high strength, as the shape of the target part is determined by the die cavity. The main conclusions are as follows:

(1) There is a critical support pressure; when the support pressure is higher than this value, the wrinkling and cross-sectional distortion defects can be suppressed completely, thereby stable bending deformation can develop. Therefore, the tube can be bent into the desired shape under the support of internal gas pressure.
(2) A theoretical prediction model of the critical support pressure is established. The results of theoretical calculation and FEM show that the critical support pressure is greatly affected by the bending radius and material properties,

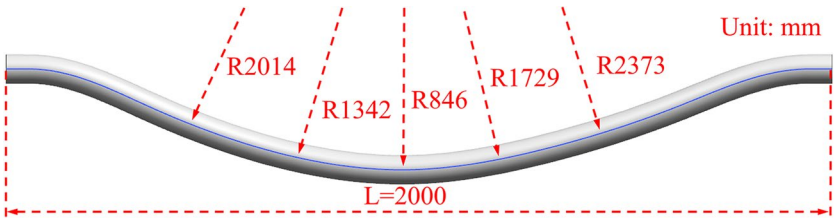

Fig. 22 3D model of a car A-pillar prebending component

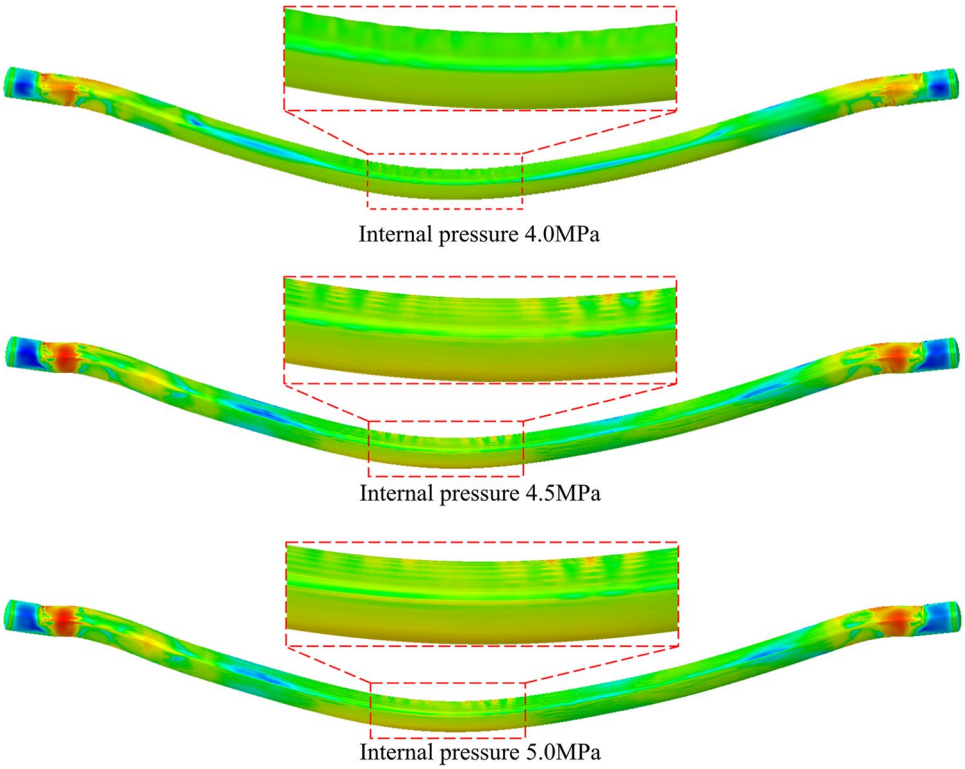

Fig. 23 FE results of prebending part with variable curvature under different support pressures

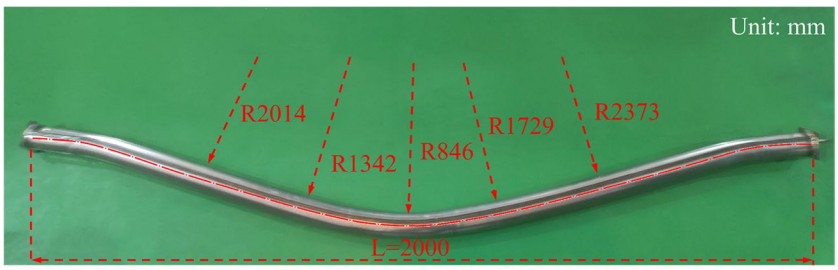

Fig. 24 A-pillar prebending component formed by the TGPB experiment

which increases with strength coefficient and decreases with bending radius and strain hardening exponent.

(3) Tubes with different curvatures or material properties are all successfully bent to the desired shape under the predicted critical support pressure. There are no wrinkles or cross-sectional distortions and little change in wall thickness. The predicted critical support pressure can be used to guide TGPB.

(4) A high-strength steel prebending component with complex variable axial curvatures has been successfully formed by TGPB technology under a support pressure of 5 MPa. The minimum and maximum bending radii of which are 846 mm and 2373 mm, respectively.

TGPB is a promising technology for tube bending. This paper only investigates the feasibility and main influencing factors of TGPB. In future studies, the effects of tube bending length, initial tube wall thickness, and die will be further investigated to gain a more systematic and in-depth understanding of TGPB.

Code availability Not applicable.

Author contribution YL: conceptualization, methodology, writing—original draft preparation, and funding acquisition. SW: writing—review, editing, software, experiment, and investigation. QQ: experiment and investigation. EX: formal analysis. ZH: supervision and funding acquisition.

Funding This study was financially supported by the National Natural Science Foundation of China (52075075) and supported by the Fundamental Research Funds for the Central Universities of China (DUT20RC(5)031) and supported by Liaoning Revitalization Talents Program (No. XLYC1802065). The authors wish to express their gratitude to the funding.

Data availability The data used to support the findings of this study are available from the corresponding author upon request.

Declarations

Ethical approval Not applicable.

Consent to participate All authors agreed to participate in this research.

Consent for publication All authors have read and agreed to the published version of the manuscript.

Competing interests The authors declare no competing interests.

References

1. Kim HY, Lim HT, Kim HJ, Lee DJ (2007) The effect of prebending on the formability in the tube hydroforming process of an aluminum rear subframe. Met Mater Int 13:87–92. https://doi.org/10.1007/BF03027557
2. Hwang YM, Manabe KI (2021) Latest hydroforming technology of metallic tubes and sheets. Metals 11:1360. https://doi.org/10.3390/met11091360
3. Lang LH, Wang ZR, Kang DC et al (2004) Hydroforming highlights: sheet hydroforming and tube hydroforming. J Mater Process Technol 151:165–177. https://doi.org/10.1016/j.jmatprotec.2004.04.032
4. Yuan SJ (2021) Fundamentals and processes of fluid pressure forming technology for complex thin-walled components. Engineering 7:358–366. https://doi.org/10.1016/j.eng.2020.08.014
5. Koç M, Altan T (2001) An overall review of the tube hydroforming (THF) technology. J Mater Process Technol 108:384–393. https://doi.org/10.1016/S0924-0136(00)00830-X
6. Yuan SJ (2012) Hydroforming processes and equipments of hollow structures with various sections. JME 48:21. https://doi.org/10.3901/JME.2012.18.021
7. Naoi H, Kitakami N, Mizumura M, Kuriyama Y (2008) Study of intrusion bending for steel tubes with thin wall thickness. J of Materi Eng and Perform 17:376–381. https://doi.org/10.1007/s11665-008-9223-7
8. Li H, Yang H, Zhan M et al (2007) Role of mandrel in NC precision bending process of thin-walled tube. Int J Mach Tools Manuf 47:1164–1175. https://doi.org/10.1016/j.ijmachtools.2006.09.001
9. Al-Qureshi HA, Russo A (2002) Spring-back and residual stresses in bending of thin-walled aluminium tubes. Mater Design 23:217–222. https://doi.org/10.1016/S0261-3069(01)00061-9
10. Kami A, Dariani BM (2011) Prediction of wrinkling in thin-walled tube push-bending process using artificial neural network and finite element method. Proc Inst Mech Eng B: J Eng Manuf 225:1801–1812. https://doi.org/10.1177/0954405411404300
11. Song P, Wang XS, Xu YC, Yuan SJ (2011) Influence of internal pressure on hydro-bending of thin-walled aluminum alloy tube. Chinese J Nonferrous Metals 21:311–317. https://doi.org/10.19476/j.ysxb.1004.0609.2011.02.010
12. Li H, Yang H, Zhan M, Kou YL (2010) Deformation behaviors of thin-walled tube in rotary draw bending under push assistant loading conditions. J Mater Process Technol 210:143–158. https://doi.org/10.1016/j.jmatprotec.2009.07.024
13. Yang H, Li H, Ma J et al (2021) Breaking bending limit of difficult-to-form titanium tubes by differential heating-based reconstruction of neutral layer shifting. Int J Mach Tools Manuf 166:103742. https://doi.org/10.1016/j.ijmachtools.2021.103742
14. Safdarian R, Kord A (2019) Experimental investigation of effective parameters in the tube rotary draw bending process. Mater Res Express 6:066531. https://doi.org/10.1088/2053-1591/ab0c36
15. Zeng YS, Li ZQ (2002) Experimental research on the tube push-bending process. J Mater Process Technol 122:237–240. https://doi.org/10.1016/S0924-0136(02)00027-4
16. Trana K (2002) Finite element simulation of the tube hydroforming process-bending, preforming and hydroforming. J Mater Process Technol 127:401–408. https://doi.org/10.1016/S0924-0136(02)00432-6
17. Taheri Kahnamouei J, Behjat B (2010) Modeling and experimental validation of the effect of sand filling on avoiding wrinkling phenomenon in thin-walled tube bending process. In: ASME 2010 10th Biennial Conference on Engineering Systems Design and Analysis, vol 4. ASMEDC, Istanbul, Turkey, pp 799–803. https://doi.org/10.1115/ESDA2010-25195
18. Strano M, Jirathearanat S, Shr S-G, Altan T (2004) Virtual process development in tube hydroforming. J Mater Process Technol 146:130–136. https://doi.org/10.1016/S0924-0136(03)00853-7
19. Lianfa Y, Cheng G (2006) A simple experimental tooling with internal pressure source used for evaluation of material formability in tube hydroforming. J Mater Process Technol 180:310–317. https://doi.org/10.1016/j.jmatprotec.2006.07.010
20. Wang XS, Song P, Zhao ZY, Yuan SJ (2011) Influence of tube ends constraint on hydro-bending of thin-walled aluminum tube. Trans Nonferrous Metals Soc China 21:s440–s444. https://doi.org/10.1016/S1003-6326(11)61621-X
21. Chen KL, Carter AJ, Korkolis YP (2022) Flange wrinkling in deep-drawing: experiments, simulations and a reduced-order model. J Manuf Mater Process 6:76. https://doi.org/10.3390/jmmp6040076
22. Chen YZ, Liu W, Zhang ZC et al (2017) Analysis of wrinkling during sheet hydroforming of curved surface shell considering reverse bulging effect. Int J Mech Sci 120:70–80. https://doi.org/10.1016/j.ijmecsci.2016.10.023
23. Chu GN, Chen G, Lin YL, Yuan SJ (2019) Tube hydro-forging – a method to manufacture hollow component with varied cross-section perimeters. J Mater Process Technol 265:150–157. https://doi.org/10.1016/j.jmatprotec.2017.11.007
24. Chu GN, Chen G, Wang GD et al (2020) Analysis of warping failure in tube hydro-forging. Int J Mech Sci 165:105216. https://doi.org/10.1016/j.ijmecsci.2019.105216
25. Wang X, Cao J (2000) Wrinkling limit in tube bending. J Eng Mater Technol 123:430–435. https://doi.org/10.1115/1.1395018
26. Yang H, Lin Y (2004) Wrinkling analysis for forming limit of tube bending processes. J Mater Process Technol 152:363–369. https://doi.org/10.1016/j.jmatprotec.2004.04.410
27. Li H, Yang H, Zhan M (2009) A study on plastic wrinkling in thin-walled tube bending via an energy-based wrinkling prediction model. Model Simul Mater Sci Eng 17:035007. https://doi.org/10.1088/0965-0393/17/3/035007
28. Wang X, Cao J (2000) On the prediction of side-wall wrinkling in sheet metal forming processes. Int J Mech Sci 42:2369–2394. https://doi.org/10.1016/S0020-7403(99)00078-8
29. Cao J, Boyce MC (1997) Wrinkling behavior of rectangular plates under lateral constraint. Int J Solids Struct 34:153–176. https://doi.org/10.1016/S0020-7683(96)00008-X
30. Cao J, Wang X (2000) An analytical model for plate wrinkling under tri-axial loading and its application. Int J Mech Sci 42:617–633. https://doi.org/10.1016/S0020-7403(98)00138-6
31. Zhang ZC, Wu JJ, Xu XL et al (2022) Mechanical modeling of tube bending considering elastoplastic evolution of tube cross-section. Materials 15:3997. https://doi.org/10.3390/ma15113997
32. Engel B, Hassan HR (2014) Investigation of neutral axis shifting in rotary draw bending processes for tubes. Steel Res Int 85:1209–1214. https://doi.org/10.1002/srin.201300333